OPTICAL CONSTANTS OF Cu_2ZnSnS_4 BULK CRYSTALS

S. Levcenko, G. Gurieva, M. Guc, and A. Nateprov

Institute of Applied Physics, Academy of Sciences of Moldova, 5, Academiei str., MD-2028, Chisinau, Republic of Moldova
E-mail: galinagurieva@gmail.com
(Received 31 March 2009)

The dielectric functions of Cu_2ZnSnS_4 bulk crystals grown by the Bridgman method were measured over the energy range 0.8 to 4.7 eV at room temperature using variable angle spectroscopic ellipsometry. The spectral dependence of complex refractive index, the absorption coefficient, and the normal-incidence reflectivity were also derived. The structure observed in the dielectric functions attributed to interband transitions E_0, E_{1A} E_{1B} has been modelled using the Adachi's model. The model parameters (strength, threshold energy, and broadening) have been determined using the simulated annealing (SA) algorithm. The results are in a good agreement with the experimental data over the entire range of photon energies.

1. Introduction

Recently, Katagiri et al. [1] have fabricated Cu_2ZnSnS_4 (CZTS)-based thin film solar cells with 6.7% in conversation efficiency using preferential etching technique. This result suggests that the CZTS-based solar cells are promising for the next generation solar cells. Cu_2ZnSnS_4 quaternary chalcopyrite semiconductor is a member of I_2-II-IV-VI_4 large class of structurally related compounds. CZTS thin films exhibit parameters optimum for solar cell materials, namely, energy gap of 1.4-1.5 eV and high optical absorption coefficient over $\sim 10^4$ cm^{-1} [2-3].

Key factors in determining the efficiency of photovoltaic devices are the optical properties of the absorber material. However, very little is known about optical constants of CZTS bulk crystals so far. The aim of the present work was to characterize the optical properties of Cu_2ZnSnS_4 bulk crystals by spectroscopic ellipsometry.

2. Experimental

Cu_2ZnSnS_4 crystals were grown by the modified Bridgman method. The energy dispersive X-ray microanalysis (EDAX) was used to measure the composition of the sample. The samples show some deviation from stoichiometry, and a sample with composition of Cu:Zn:Sn:S as 21.9:16.0:13.1:49.0 at %, respectively, was used for the optical study The structural analysis was performed by X-ray diffraction. The ingots grown show the polycrystalline phase, presenting as dominant kesterite structure, with indication on some of binaries like SnS.

The optical measurements were carried out with a variable-angle spectroscopic ellipsometer at room temperature in the photon energy range from 0.8 to 4.7eV, at two incidence angles Φ, 60° and 70°, to ensure a consistent and accurate determination of the dielectric function of the compounds. A special attention was paid to the preparation of good quality "pure" surface as was proposed by Albornoz et al. [4]. The real and imaginary parts of the dielectric function $\varepsilon(\omega) = \varepsilon_1(\omega) + i\varepsilon_2(\omega)$ may thus be obtained from the equation of two-phase (substrate-ambient) model [1]

$$\varepsilon = \sin^2 \Phi \left[1 + \tan^2 \Phi \left(\frac{1-\rho}{1+\rho} \right)^2 \right], \quad (1)$$

where Φ is the incidence angle of the photon beam and ρ is the complex ratio of the Fresnel coefficients explained in reference [4].

3. Theoretical model

Adachi's model dielectric function (MDF) describes features of the complex dielectric function $\varepsilon(E)$ of a crystalline material by electronic transitions between bands in the neighborhood of critical points (CPs) assuming the bands are parabolic. It is well known that the optical transitions are strongly affected by a damping effect (lifetime broadening). This effect is accounted for MDF via phenomenological replacing E by $E+i\Gamma$ in the expressions for $\varepsilon(E)$, where Γ is broadening parameter associated with each interband transition. The MDF method successfully applied to model the dielectric function and the optical constants of zinc-blende semiconductors II-VI [5, 6], I-II-VI_2 [7, 8]. The complex dielectric function of Cu_2ZnSnS_4 was described, as for materials I-III-VI_2, by the sum of three terms, $\varepsilon_0(E)$, $\varepsilon_1(E)$, and $\varepsilon_{1\infty}$ corresponding, respectively, to the one-electron contributions at the E_0 and $E_{1\beta}$ critical points, where $\beta = A, B$ refers to different energy transitions after the main one and the additive constant

$$\varepsilon(E) = \varepsilon_0(E) + \varepsilon_1(E) + \varepsilon_{1\infty}. \quad (2)$$

The first term $\varepsilon_0(E)$ corresponding to fundamental gap E_0 is assigned to the three-dimensional (3D) M_0 critical point

$$\varepsilon_0(E) = AE_0^{-3/2}\chi_0^{-2}(2-(1+\chi_0)^{1/2}-(1-\chi_0)^{1/2}) \quad (3)$$

with $\chi_0=(E+i\Gamma)/E_0$, here A and Γ are the strength and the damping energy of the E_0 gap, respectively.

The second term corresponding to the higher critical-points $E_{1\beta}$ (β=A, B) is assigned to the two-dimensional (2D) critical points and is given by

$$\varepsilon_1(\mathrm{E}) = \frac{C}{(1-\chi^2)-i\chi\gamma} \text{-} \mathrm{B}_{1\mathrm{B}}\chi_{1\mathrm{B}}^{-2} Ln(1-\chi_{1\mathrm{B}}^{\ 2}) \quad (4)$$

with $\chi = E/E_{1A}$, $\chi_{1B}=(E+i\Gamma_{1B})/E_{1B}$, where $B_{1B}(C)$, $\Gamma_{1\beta}(\gamma)$ are the strengths and damping constants of the E_{1A} and E_{1B} transitions, respectively.

The including of an additional term $\varepsilon_{1\infty}$ to $\varepsilon_1(E)$ improves the fit of experimental data [5-9]. This term contains contribution of higher lying interband transitions. The $\varepsilon_{1\infty}$ parameter may take second order polynomial of photon energy [9] or even to be constant [5, 6] in the spectral range. In our calculation, this parameter was used as constant.

The unknown parameters of optical transitions entering Eq. (2) are adjusted using simulated annealing (SA) algorithm [10] so as to obtain the best fit on experimental spectra $\varepsilon(E)$ through the minimization of the following objective function [8]

$$f = \sum_{i=1}^{N} \left(\left| \frac{\varepsilon_1(E_i)}{\varepsilon_1^{\mathrm{expt}}(E_i)} - 1 \right| + \left| \frac{\varepsilon_2(E_i)}{\varepsilon_2^{\mathrm{expt}}(E_i)} - 1 \right| \right)^2, \quad (5)$$

where N is the number of photon energies at which $\varepsilon(\omega)$ were measured, and $\varepsilon_1^{\mathrm{expt}}(E_i)$, $\varepsilon_1(E_i)$ $\varepsilon_2^{\mathrm{expt}}(E_i)$, $\varepsilon_2(E_i)$ are the experimental and calculated values of the real and imaginary parts of complex dielectric function at E_i point, respectively.

4. Results and discussion

The measured dielectric function $\varepsilon(E) = \varepsilon_1(E) + i\,\varepsilon_2(E)$ for Cu_2ZnSnS_4 obtained from Eq. (1) is shown in Fig. 1 where solid squares represent experimental data. As one can see, the spectra exhibit several critical-point structures. The energy threshold of the fundamental absorption edge $E_0=E_g$ well identified in Fig. 1 may correspond to direct transition from the valence band maximum to the conduction band minimum at the center of the Brillouin zone (BZ, Γ point). The second E_{1A} and third energy thresholds E_{1B} appear in the region below 3.0 and 4.4 eV. Band structure calculation needed to perform identifications of the energy transitions observed is not available for Cu_2ZnSnS_4 but is well known for $CuInS_2$ [11]. Assuming that the origin of interband transitions in Cu_2ZnSnS_4 is the same as in $CuInS_2$, the E_{1A} and E_{1B} transitions can be attributed to transitions at the N point in the BZ [11].

The Adachi's MDF was applied to calculate the dielectric function as well as the optical constants of the studied crystal. The resulting analytical lines from the best fits of the experimental data in Fig. 1 have been obtained considering CPs of the three-dimensional-type 3D in the E_0 region and of the type 2D $M_1(M_0)$in the E_{1A} (E_{1B}) region Eq. (3) and (4), respectively.

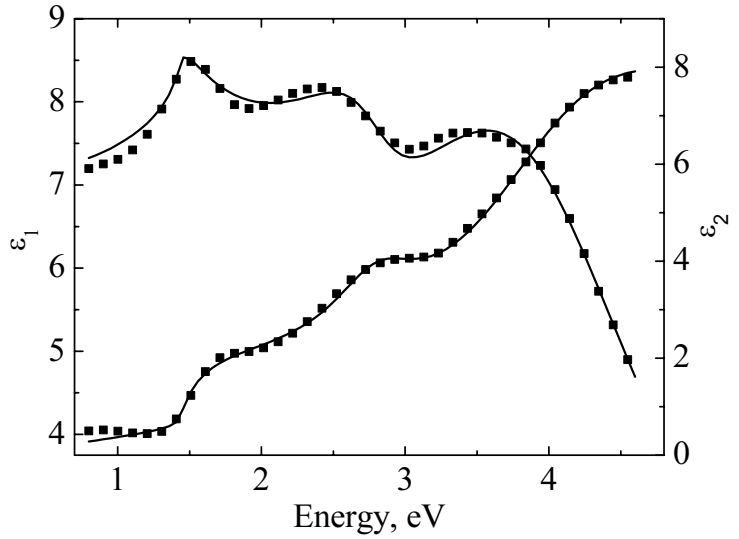

Fig. 1. $\varepsilon(E)$ spectra of Cu_2ZnSnS_4: measured (squares) and calculated (solid line) using SA algorithm. The fit determined CP parameters are listed in Table I.

The model parameters A, B, C, E_0, E_{1A}, E_{1B}, and $\Gamma(\gamma)$ of studied sample are calculated using the SA algorithm are gathered in Table II. A good agreement between our calculations and the experimental data can be observed (Fig. 2). As an indication of the accuracy with respect to the experimental values, the relative errors lying below the 1.5% and 2.6% for the real and the imaginary parts, respectively, have been calculated for the studied material (Table I). The deduced values of E_0 =1.44 eV at room temperature are in agreement with the E_g obtained from absorption measurements for thin films [2, 3].

Table I. Model parameter values.

Parameters	E_0(eV)	Γ_0(eV)	A(eV$^{1.5}$)	E_1(eV)	γ_1	C_1	E_{2A}(eV)	Γ_2(eV)	B_{2A}	$\varepsilon_{1\infty}$	error	
											ε_1%	ε_2%
Cu_2ZnSnS_4	1.44	0.03	6.67	2.82	0.27	0.33	3.86	0.83	5.62	0.30	1.45	2.55

The optical constants of interest, namely, the complex refractive index $n^*=n+ik$, the normal-incidence reflectivity R, and the absorption coefficient α, can be readily computed from well known equations. Figure 2 shows the spectral dependence of α and R for and Cu_2ZnSnS_4 crystal.

The experimental spectral dependences of n and k, as well as the ones calculated using the Adachi's MDF and the SA algorithm, are presented in Fig. 3 for Cu_2ZnSnS_4. A good agreement is observed for studied samples.

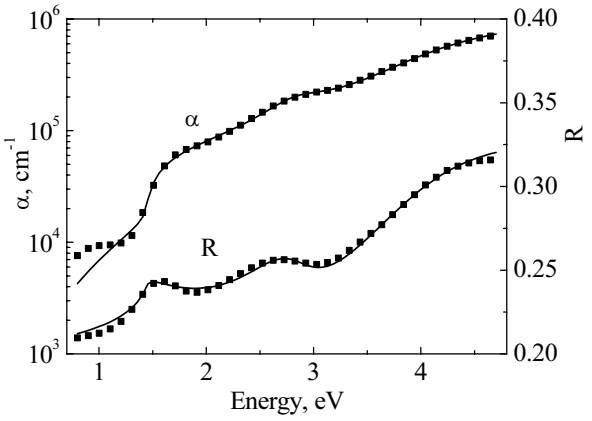

Fig. 2. Spectral dependence of the absorption coefficient (α) and normal-incidence reflectivity (R) for Cu_2ZnSnS_4: experimental (squares) and numerically calculated (solid lines) using the MDF model and the SA algorithm.

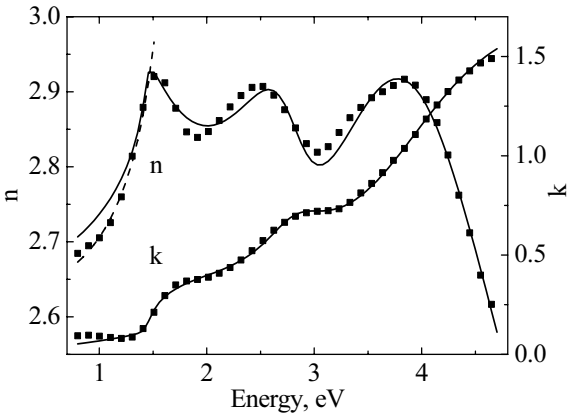

Fig. 3. Spectral dependence of the real refraction index (n) and extinction coefficient (k) for Cu_2ZnSnS_4: experimental (squares) and numerically calculated (solid lines) using the SA algorithm. The dashed line shows the result calculated by Eq. (6).

The experimental n data have also been analyzed using a simple theoretical model, namely, the first-order Sellmeier's equation [12]

$$n^2(\lambda) = A + \frac{\lambda^2}{\lambda^2 - B}, \tag{6}$$

where A and B are the fitting parameters. The dashed line in Fig. 3 represents the fitting of Eq. (6) to the experimental data. The values of the fitting parameters A and B are 5.92 and 0.44, respectively. As $\lambda \to \infty$, the electronic contribution to the dielectric function approaches the limiting value ε_∞, i. e., the high-frequency dielectric constant. The value of $\varepsilon_\infty = n^2 (\lambda \to \infty) = A+1$ is about 6.92 for Cu_2ZnSnS_4. This value in a good agreement with prediction of MDF model of ε (E) in the infrared region from Eq. (2) ε ($E \to 0$) is about 7.09. The reported value for $CuInS_2$ is 6.7 [13].

5. Conclusions

We have reported the dielectric function of Cu_2ZnSnS_4 bulk crystals measured by spectroscopic ellipsometry at room temperature. The spectral dependence of the real and imaginary parts of the complex dielectric function for Cu_2ZnSnS_4 crystals are modelled in the 0.8-4.7 eV photon energy range using Adachi's MDF model for the optical properties of semiconductors and the simulated annealing algorithm. A good agreement with the experimental data is obtained and the model parameters (strength, threshold energy, and broadening) have been determined. Optical constants, such as the complex refractive index, extinction and ab-

sorption coefficients, and normal-incidence reflectivity, are also presented. Both spectral dependences of the optical constants and the critical point analysis are expected to be useful in studies of solar cells and other devices based on these materials.

Acknowledgments

Financial support from project ASM-BMBF 09.820.05.07 is acknowledged.

References

[1] H. Katagiri, K. Jimbo, S. Yamada, T. Kamimura, W.S. Maw, T. Fukano, T. Ito, and T. Motohiro, Applied Physics Express, 1, 041201, (2008).
[2] K. Ito and T. Nakazawa, Jpn. J. Appl. Phys., 27, 2094, (1988).
[3] H. Katagiri, Thin Solid Films, 426, 480, (2005).
[4] J.G. Albornoz, R. Serna, and M. Leon, J. Appl. Phys., 97, 103515, (2006).
[5] S. Adachi and T. Taguchi, Phys. Rev. B, 43, 9569, (1991).
[6] S. Adachi and E. Herbert Li, J. Appl. Phys., 68, 1192, (1990).
[7] T. Kawashima, S. Adachi, H. Miyake, and K. Sugiyama, J. Appl. Phys., 84, 5202, (1998).
[8] A.B. Djurisic and E.H. Li, Appl. Phys. A, 73, 189, (2001).
[9] C.C. Kim, J.W. Garland, H. Abad, and P.M. Raccah, Phys. Rev. B, 45, 11749, (1992).
[10] A. Corana, M. Marchesi, C. Martini, and S. Ridella, ACM T. Math. Software, 13, 262, (1987).
[11] M.I. Alonso, K. Wakita, J. Pascual, M. Garriga, and N. Yamamoto, Phys. Rev. B, 63, 075203, (2001).
[12] J.I. Pankove, Optical Processes in Semiconductors, Dover, New York, 103, 1971.
[13] N.N. Syrbu, I.M. Tiginyanu, L.L. Nemerenko, V.V. Ursaki, V.T. Tezlevan, and V.V. Zalamai, J. Phys. Chem. Sol., 66, 1974, (2005).